Characterization and Structure Analysis of PLGA/Collagen Nanofibrous Membranes by Electrospinning

Jong-Seok Park,[1] Jong-Bae Choi,[1] Sun-Young Jo,[1] Youn-Mook Lim,[1] Hui-Jeong Gwon,[1] Myung Seob Khil,[2] Young-Chang Nho[1]

[1]*Radiation Research Division for Industry and Environment, Korea Atomic Energy Research Institute, 1266 Sinjeong-dong, Jeongeup-si, Jeollabuk-do 580-185, Republic of Korea*
[2]*Department of Organic Materials and Fibers Engineering, Chonbuk National University, Jeongju 561-756, Republic of Korea*

Received 27 June 2011; accepted 17 January 2012
DOI 10.1002/app.36833
Published online in Wiley Online Library (wileyonlinelibrary.com).

ABSTRACT: Poly(DL-lactide-*co*-glycolide) (PLGA)/marine collagen nanofibrous membranes (PCNMs) with different weight ratio of PLGA to collagen were fabricated by an electrospinning method. The morphology and diameter distribution of electrospun nanofibers were investigated by scanning electron microscopy (SEM). SEM images showed that the morphology and diameter distribution of the nanofibers were mainly affected by the concentration of the solution, weight ratio of the PLGA/collagen, and applied electric voltage, respectively. To investigate the cell responses, MG-63 cells isolated from a human mandible were cultured onto various substrates and their adhesion, spreading, and proliferation were examined. Immunofluorescent staining of MG-63 cultured on the PCNMs demonstrated homogeneous localization of F-Actin and vinculin in their cytoplasms. However, no mature adhesive structures were observed in the cell cultured on other substrates. Also, the cells seeded on the materials proliferated. These results suggest that PCNMs strongly support the attachment and growth of osteosarcoma cells. © 2012 Wiley Periodicals, Inc. J Appl Polym Sci 000: 000–000, 2012

Key words: nanofiber; PLGA; biocompatibility material; electrospinning

INTRODUCTION

The fundamental goal of tissue engineering is to develop biological substitutes that restore, maintain or improve diseased, injured, or congenitally absent tissues or organs.[1] Strategies for the engineered reconstitution of tissues and organs are typically centered on three fundamental approaches: cell-based therapy, scaffold-based therapy, or bioactive molecule-based therapy.[2] Among these types of approaches, biological achievements regarding cell cultures using biodegradable materials are more promising techniques.

Fiber-based porous scaffolds, which structurally mimic an extracellular matrix (ECM), have been generated from numerous natural or synthetic biopolymers, such as lyophilized elastin–collagen, accellularized aortic elastin and collagen, poly(ether-ether-ketone)/-hydroxyapatite biocomposites, and chitosan-based materials. All of these scaffolds are biocompatible, and enhance cell *in vitro* growth.

Recent studies have demonstrated the usefulness of electrospinning as a platform technology for generating fibrous scaffolds for tissue engineering purposes. Various biodegradable synthetic polymers,[3] peptide copolymers,[4] and natural proteins[5] have been electrospun into micro/nanofibers for a multitude of biomedical applications such as scaffolds used in tissue engineering,[6] wound dressing,[7] drug delivery,[8] and vascular grafts.[9] This process involves the use of an electric field to eject a polymer fiber from the solution to the collector. The fiber deposits randomly to form a fused fiber mesh, and the fiber diameter can be controlled over a range of 100 nm to 5 mm by varying the electrical potential, throw distance, needle diameter, and solution concentration.[10] Importantly, the range of fiber diameters that can be achieved are two to three orders of magnitude smaller than those formed by conventional extrusion[11] and wet spinning[12] processes, and includes the range of feature sizes known to induce contact guidance.

In general, synthetic biodegradable polymers (e.g., poly(lactide-*co*-glycolide (PLGA)) are easily formed into desired shapes with good mechanical strength, and their degradation time scales can be estimated.[13] Despite these advantages, the scaffolds derived from synthetic polymers are insufficient for cell-recognition signals, and their hydrophobic properties

Correspondence to: Y.-C. Nho (jaspa@hanmial.net).
Contract grant sponsor: Ministry of Education, Science and Technology, Korea (Nuclear R&D program through the Korea Science and Engineering Foundation).

obstruct cell seeding. In contrast, naturally derived polymers have the potential advantages of specific cell interactions and a hydrophilic nature but possess poor mechanical properties.

Collagen, one of the main classes of structural ECM proteins, has been used as a biomaterial in a variety of tissue applications because of its excellent biocompatibility, low antigenicity, high biodegradability, good hemostatic qualities, and cell-binding properties.[14] Also, electrospinning of soluble collagen is a suitable method to prepare scaffolds with high porosity and surface area for tissue engineering of small diameter vessels.[15,16]

In this article, we report the preparation and characterization of PLGA/collagen nanofibers obtained by electrospinning. The effects of solution concentration, weight ratio of the PLGA/collagen, applied electric voltage, solution flow rate, and needle size on the morphology and average size of the electrospun PLGA/collagen fibers were also investigated. We also investigated the growth and phenotype of MG-63 cultured on PLGA/collagen scaffolds.

EXPERIMENTAL

Materials

The PLGA, LA:GA = 50 : 50) was received from Boehringer Ingelheim Pharma GmbH, KG. Marine collagen was prepared as described in our previous article.[17] HFIP (1,1,1,3,3,3-Hexafluoro-2-propanol) was purchased from Sigma–Aldrich.

Preparation and properties of polymer solution

The concentration of PLGA and collagen in the solutions was varied from 5 to 20 wt %. The weight ratios of PLGA and collagen in the mixed solutions were either 3 : 7, 5 : 5, or 7 : 3. Various polymer solutions were prepared at room temperature by dissolving the PLGA and collagen in HFIP, and stirred by magnetic force to speed up the dissolution process. The solution viscosities were determined by a Brookfield DV-II viscometer with a rotational speed of 100 rpm at 25°C.

Electrospinning process

The electrospinning setup used in this study consisted of a syringe and needle, an aluminum collecting drum, and a high voltage supply. The high-voltage electric field used for the electrospinning process was produced by a controllable high-voltage power supply (DC-high-voltage generator, Model cps-40KO3VIT, CHUNGPA EMT.). The polymer solution was placed in a 10-mL syringe attached to a needle and the syringe was fixed at the front face of the collector (aluminum drum). The polymer solution formed a droplet at the tip of the syringe due to its weight and surface tension. The anode of the high-voltage power supply was connected to a copper wire, which was immersed in the polymer solution. The cathode was connected to the aluminum plate. By applying voltage between the anode and cathode, the droplet was instantly disintegrated into fibers that eventually deposited onto the aluminum plate. The needle sizes were 18, 23, and 27 G (0.0330, 0.0125, and 0.0075 in), respectively. The polymer solution was electrospun at positive voltages of 5, 10, 15, and 20 kV, with a working distance of 14 cm (the distance between the needle tip to collector). The mass flow rates of the PLGA/collagen solution were 0.001, 0.003, and 0.005 mL/min, for the tree needle lengths, respectively.

Morphology

The morphology of the electrospun PLGA/collagen fibers was observed using a scanning electron microscope (JSM-5200). The diameters of the electrospun fibers were measured from the SEM pictures.

Cell and cell culture

The MG-63 cells were derived from a human osteosarcoma of a 14-year-old Caucasian male (Korean Cell Line Bank, KCLB) and cultured in DMEM (Dulbecco's Modified Eagle Medium, Gibco, USA) containing 10% FBS (Fetal Bovine Serum, Gibco, USA) and 1% PS (Penicillin-Streptomycin, Gibco, USA). The cells were incubated at 37°C in a humidified atmosphere with 5% CO_2.

Cell adhesion

To investigate cell adhesion and morphology, the prepared PCNMs were placed in a six-well cell culture plate (Nunc, Denmark) and sterilized by gamma-rays at an irradiation dose rate of 10 kGy/h for 2.5 h. To seed the MG-63 cells onto the PCNMs, 0.2 mL of a suspension containing 2.5×10^3 cells/mL was dispersed onto PCNMs for a homogenous distribution of cells and then incubated for 4 h at 37°C. Following incubation, the samples were added to 0.3 mL of the culture medium. After 3 days, the samples were observed by an optical microscope (Leica, Germany) and visualized through immunofluorescent staining.

Analytical assays

Cell-cultured PCNMs were fixed in 2.5% (v/v) glutaldehyde for 4 h at 4°C, respectively, followed by dehydration with a graded ethanol series and freeze-

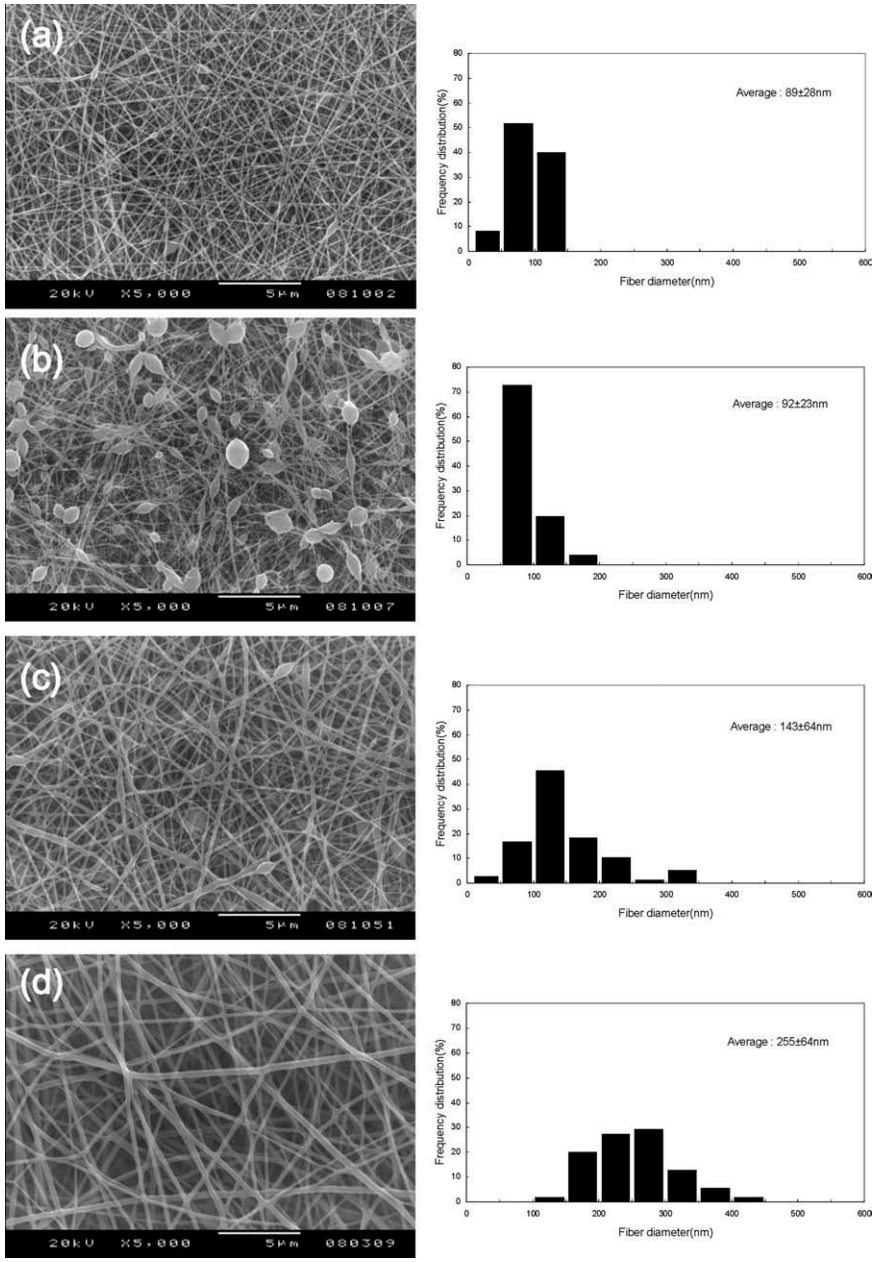

Figure 1 SEM images and fiber diameter of PLGA/collagen fibers as a function of the polymer solution concentration (PLGA/collagen = 7/3 (w/w), electric voltage = 15 kV, flow rate = 0.003 mL/min, tip-target distance = 14 cm, needle size = 27 G); (a) concentration = 5 wt %, (b) concentration = 10 wt %, (c) concentration = 15 wt %, and (d) concentration = 20 wt %.

drying (24 h). The dried specimens were coated with gold and the cell alignment was observed by SEM measurement. For histological analysis, cell-polymer constructs were stained with hematoxylin and eosin (H&E) for the nucleus and cytoplasm.

Immunofluorescence staining

Cell-cultured PCNMs were washed in DPBS (Dulbecco's Phosphate Buffered Saline, Gibco, USA) and fixed in 4% (v/v) paraformaldehyde (Aldrich, USA) for 10 min at RT (room temperature). After rinsing in PBS, the samples were permeabilized in a cyoskeletal buffer (10.3 g sucrose, 0.292 g NaCl, 0.06 g $MgCl_2$, 0.476 g HEPES buffer, 0.5 mL Triton X-100,

TABLE I
Viscosity of PLGA/Collagen Solutions as a Function of the Solution Concentration

Concentration (wt %)	PLGA/collagen	Viscosity (c_p)
5	7/3	5
10	7/3	24
15	7/3	96
20	7/3	192

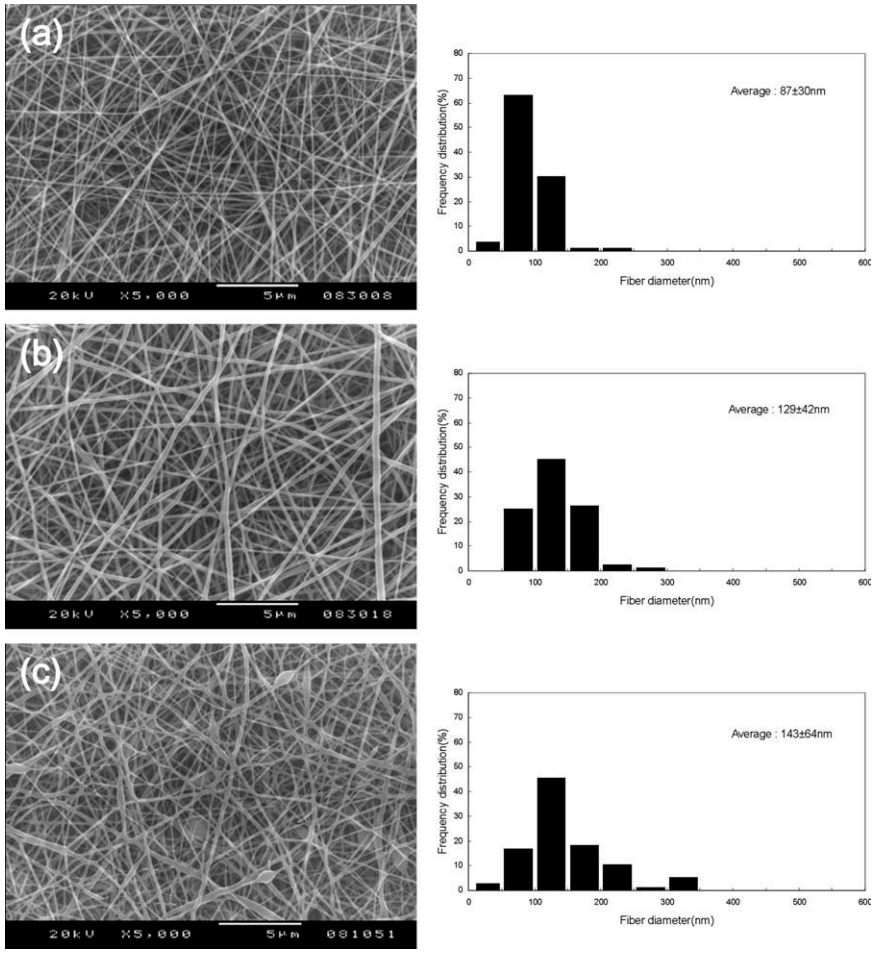

Figure 2 SEM images and fiber diameter of PLGA/collagen fibers as a function of the PLGA/collagen ratio (concentration = 15 wt %, electric voltage = 15 kV, flow rate = 0.003 mL/min, tip-target distance = 14 cm, needle size = 27 G); (a) PLGA/collagen = 3/7 (w/w), (b) PLGA/collagen = 5/5 (w/w), and (c) PLGA/collagen = 7/3 (w/w).

in 100 mL water, pH 7.2) for 10 min at 4°C. The samples were washed in PBS and blocked with 10% FBS for 1 h at 37°C. The samples were washed with PBS and incubated with 5 Ug/mL of anti-vinculin (Upstate, USA) for 40 min at RT. The samples were rinsed with PBS and incubated with Hoechst 33258 pentahydrate (Invitrogen, USA), rhodamine-phalloidin (Invitrogen, USA), and Alexa-fluoro 488 rabbit anti-mouse IgG (Invitrogen, USA) for 40 min at RT in the dark. The samples were washed in PBS. Following mounting, they were examined immediately using a fluorescence microscope (Leica, Germany).[18–20]

RESULTS AND DISCUSSION

Electrospinning of PLGA/collagen

The preparation of PLGA/collagen nanofibrous membrane by electrospinning is very desirable because collagen and PLGA were widely used in a variety of tissue engineering applications.[21,22] Huang et al.[23] reported electronspun collagen dissolved in acetic acid aqueous solution and Mao and Coworkers[24] reported electronspun PLGA dissolved in tetrahydrofuran (THF) and dimethylformamide (DMF) to prepare the continuous PLGA nanfibers.

In this study, continuous PLGA/collagen nanofibers in the HFIP solutions were obtained and the effects of solution concentration, weight ratio of the PLGA/collagen, applied electric voltage, solution flow rate, and needle size on the morphology and average size of the electrospun PLGA/collagen fibers were also investigated. Varying the solution concentration alters the morphology of the nanofibers formed (Fig. 1). At a low concentration, the fibers have an irregular, undulating morphology. At a high concentration, the nanofibers have a regular, cylindrical morphology with a larger diameter on average. The viscosity of the polymer solutions are summarized in Table I. The viscosity increased with an increase in the concentration (5–20 wt %) of the polymer solution. The effect of PLGA/collagen ratio on the average diameter of electrospun nanofibers is quantified in Figure 2. The average diameter of

TABLE II
Viscosity of PLGA/Collagen Solutions as a Function of the PLGA/Collagen Ratio

Concentration (wt %)	PLGA/Collagen	Viscosity (c_p)
15	3/7	48
15	5/5	72
15	7/3	96

electronspun nanofibers increased with the content of PLGA. The key point of this result is presented in Table II. Table II shows a change in viscosity depending on the PLGA/collagen ratio. Increasing the PLGA ratio increased the viscosity. At a higher viscosity, the nanofibers have a larger diameter. This result is very similar to that of Figure 1 and Table I.

Viscosity plays an important role in determining the range of concentrations from which continuous fibers can be obtained during electrospinning. Below a certain concentration, drops will form instead of fibers. In electrospinning, the coiled macromolecules in solution were transformed by the elongational flow of the jet into oriented entangled network that persist with fiber solidification. At low viscosities, the surface tension is the dominant effect on fiber morphology. Below this concentration, chain

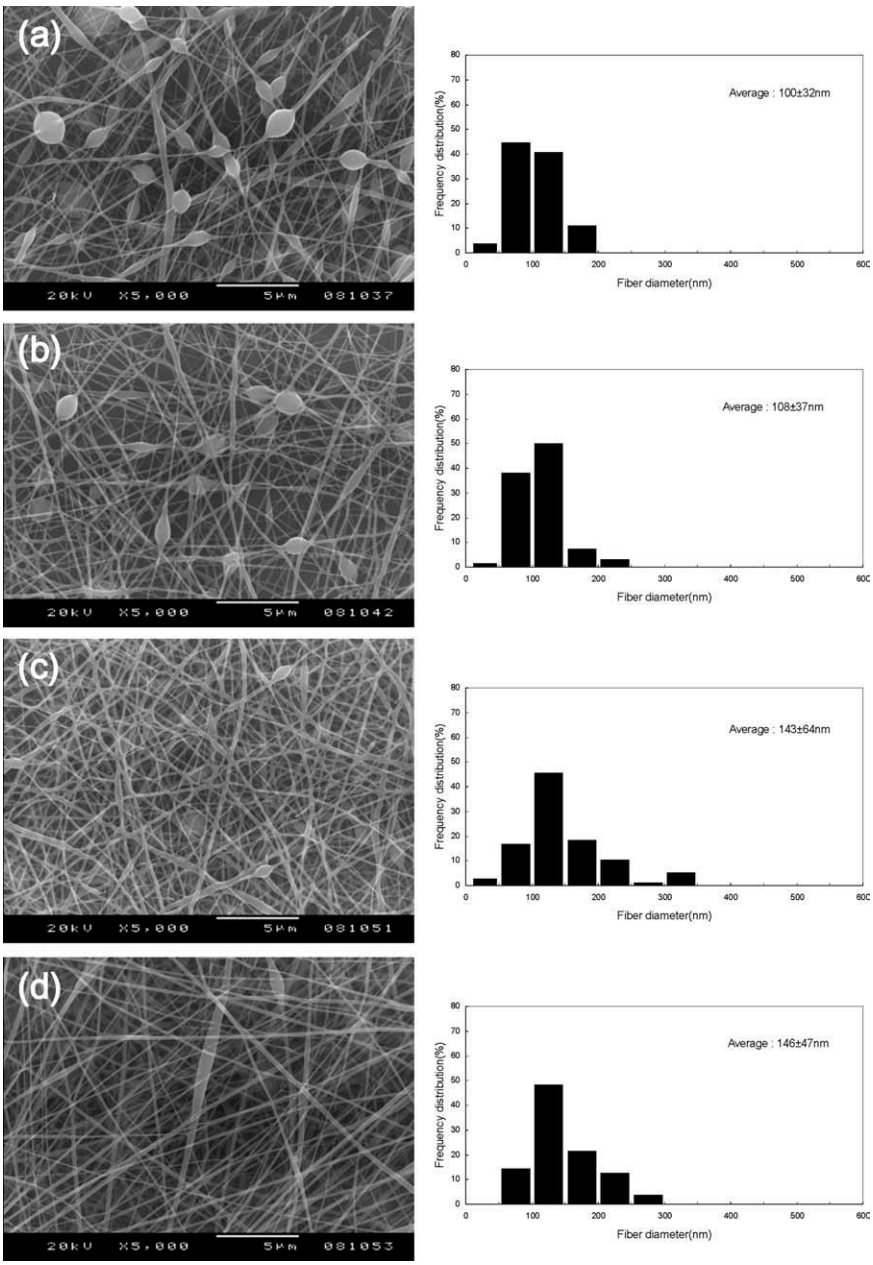

Figure 3 SEM images and fiber diameter of PLGA/collagen fibers as a function of the electric voltage (concentration = 15 wt %, PLGA/collagen = 7/3 (w/w), flow rate = 0.003 mL/min, tip-target distance = 14 cm, needle size = 27 G); (a) electric voltage = 5 kV, (b) electric voltage = 10 kV, (c) electric voltage = 15 kV, and (d) electric voltage = 20 kV.

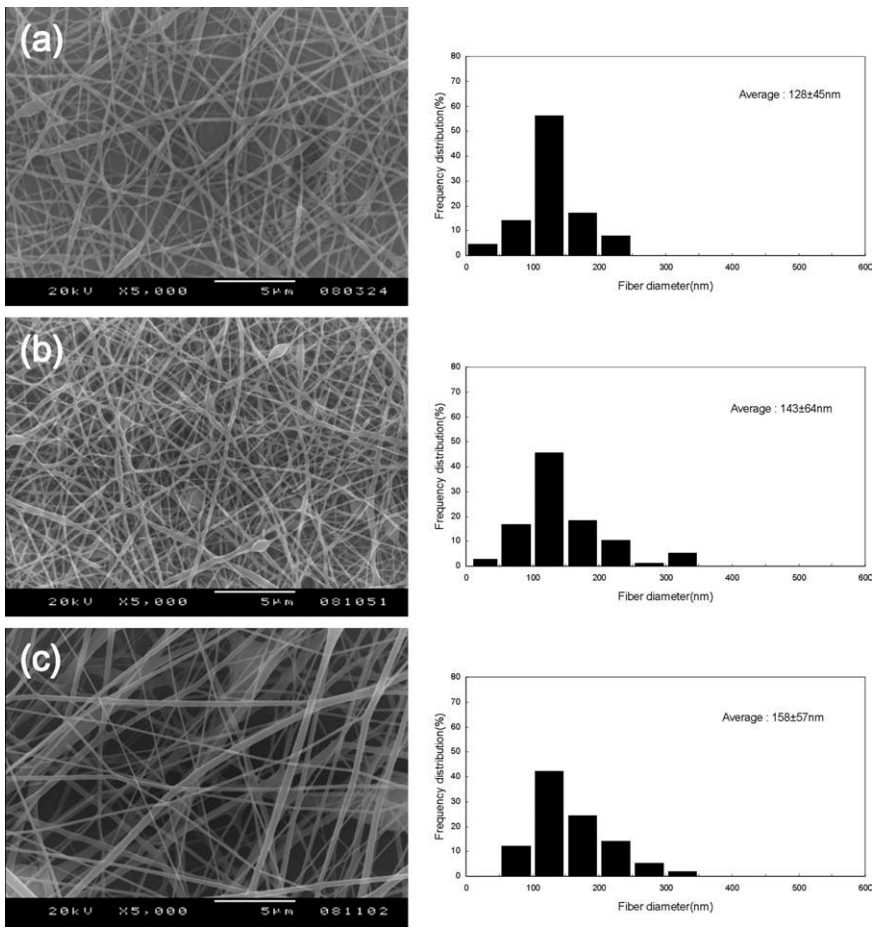

Figure 4 SEM images and fiber diameter of PLGA/collagen fibers as a function of the flow rate (concentration = 15 wt %, PLGA/collagen = 7/3 (w/w), electric voltage = 15 kV, tip-target distance = 14 cm, needle size = 27 G); (a) flow rate = 0.001 mL/min, (b) flow rate = 0.003 mL/min, and (c) flow rate = 0.005 mL/min.

entanglements were insufficient to stabilize the jet and contraction of the diameter of the jet driven by the surface tension caused the solution to form beads or beaded fibers. At high concentrations, the processing will be prohibited by an inability to control and maintain the flow of the polymer solution to the tip of the needle and by the cohesive nature of the high viscosity. Viscoelastic force which resisted rapid changes in fiber shape resulted in uniform fiber formation. However, it was impossible to electrospin if the solution concentration or the corresponding viscosity was too high due to the difficulty in liquid jet formation. From these result, it is found that the viscosity of the solution plays an important role in determining the diameter of nanofiber during electrospinning.

A series of experiments were carried out when the applied voltage was varied from 5 to 20 kV and the tip to target distance was held at 14 cm. The results are shown in Figure 3. There was a slight increase in the average fiber diameter with an increase in the applied electric field. A narrow distribution of the fiber diameter was observed at a lower voltage of 10 kV, while a broad distribution in the fiber diameter was obtained at higher applied voltages of 10–20 kV. At low voltages, a drop is typically suspended at the needle tip, and a jet will originate from Taylor cone producing bead-free spinning. As the voltage is increased, the volume of the drop at the tip decreases, causing the Taylor cone to recede. The jet originates from the liquid surface within the tip, and more beading is seen. As the voltage in increased further, the jet eventually moves around the edge of the tip, with no visible Taylor cone, at these conditions, the presences of many beads can be observed.[25] This results in an increase of the fiber diameter. Corona discharge was observed at voltages above 20 kV, making electrospinning impossible.

Figure 3 also showed that the morphology was changed from a beaded fiber to a uniform fiber. The bead morphology is correlated with the shape of the liquid surface from where the jet originated. The change in the shape of the liquid surface reflects a change in the mass balance that occurs at the end of the capillary tip. Increasing the voltage causes the rate at which the solution is removed from the

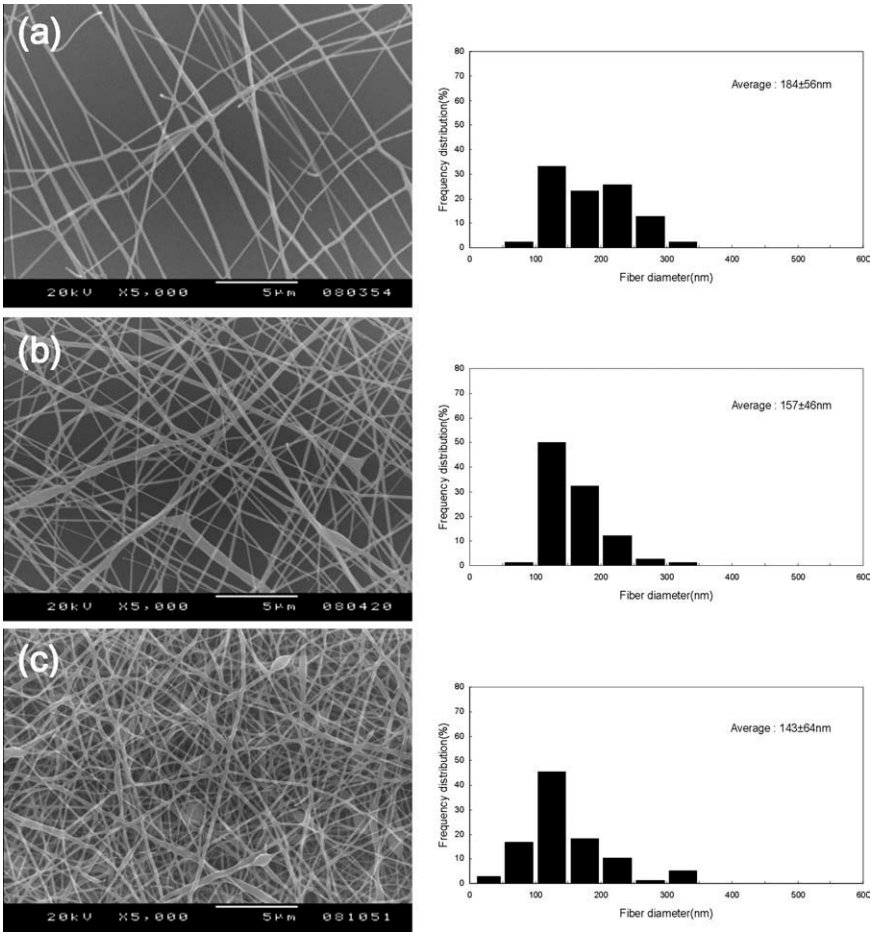

Figure 5 SEM images and fiber diameter of PLGA/collagen fibers as a function of the needle size (concentration = 15 wt %, PLGA/collagen = 7/3 (w/w), electric voltage = 15 kV, flow rate = 0.003 mL/min, tiptarget distance = 14 cm); (a) needle size = 18 G (0.0330 in), (b) needle size = 23 G (0.0125 in), and (c) needle size = 27 G (0.0075 in).

capillary tip to exceed the rate of delivery to the tip needed to maintain the conical shape of the surface. Fiber bead density increases with an increase in the instability of the jet at the spinning tip.

Figure 4 shows the SEM images and fiber diameter of PLGA/collagen fibers as a function of the flow rate. As shown in Figure 4, there was a significant increase in the fiber diameter with an increased flow

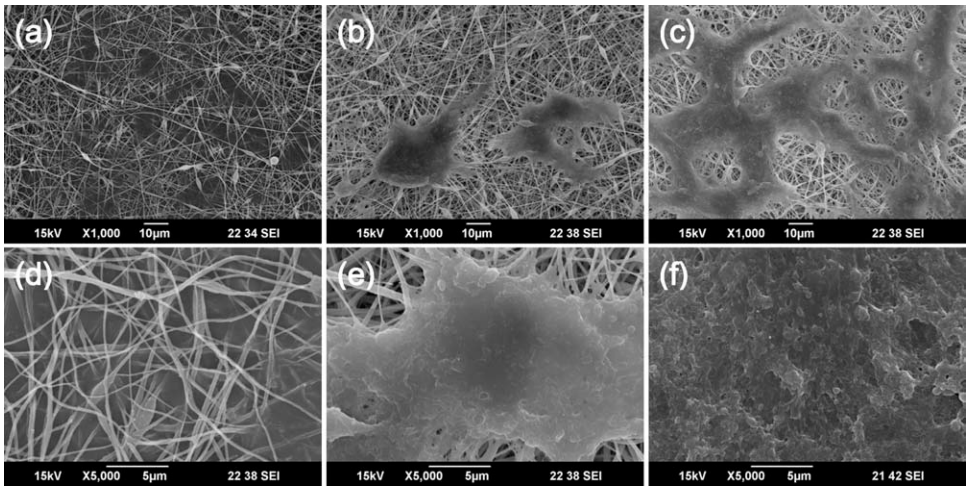

Figure 6 SEM images of MG-63 in PCNMs: (a,b,c) 3, 7, and 10 days after cell seeding (×1000), (d,e,f) 3, 7, and 10 days after cell seeding (×5000).

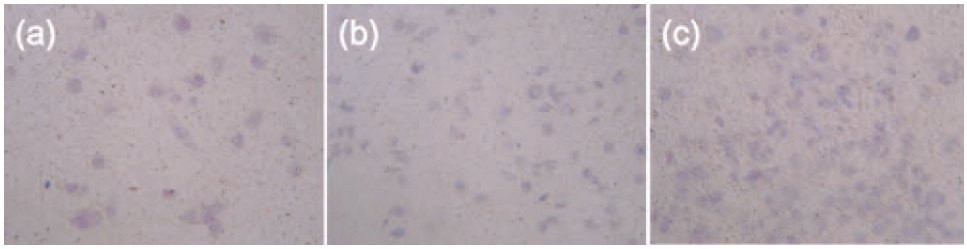

Figure 7 H&E stains of MG-63 in PCNMs: (a) 3 days, (b) 7 days, and (c) 10 days after cell seeding. [Color figure can be viewed in the online issue, which is available at wileyonlinelibrary.com.]

rate. When the flow rate exceeded a critical value, the delivery rate of the solution jet to the capillary tip exceeded the rate at which the solution was removed from the tip by the electric forces. This shift in the mass-balance resulted in sustained but unstable jet and fibers with broad distribution in the fiber diameter were formed.

Also, the change of fiber diameter by changing the needle size (needle tip diameter) is shown in Figure 5. By increasing the needle size, the average fiber diameter was increased. The probable reason for this result is that the change of the needle size could change the flow rate. This result is very similar to that of Figure 4. As the need size is increased, more solution was drawn from the tip of the needle and the average diameter of nanofiber increased. As a result, the average diameter of nanofiber increased with the needle size resulted in a higher flow rate.

Cell adhesion on the PCMNs films

Electrospun nanofibrous membranes provided a high level of specific surface area for cells to attach and proliferate. MG-63 was seeded for 3, 7, and 10 days in PCNMs and analyzed using SEM. The results showed apparent morphological differences (Fig. 6). Ten days after cell seeding, MG-63 apparently elaborated a substantial amount of extracellular matrices [Fig. 6(c,f)], in comparison with MG-63 a seeded for 3 and 7 days [Fig. 6(a,d) and Fig. 6(b,e), respectively]. MG-63 showed a somewhat rounded shape after 3 days cell seeding [Fig. 6(a,d)] in contrast to the more elongated cell shape that appeared after 10 days cell seeding [Fig. 6(c,f)], suggesting MG-63 attachment to PCNMs. As a result, the electrospun composite membranes could mimic the natural ECM and positively promote cell–matrix and cell–cell interactions.

H&E staining of MG-63 cell seeding revealed their near confluence (Fig. 7). The numbers of spread cells were increased as the days passed. By 10 days after cell seeding, MG-63 apparently showed random orientations among PCNMs [Fig. 7(c)]. H&E image analysis corroborated significant trends in cell number. Also, while the MG-63 microintegration results obtained were very promising in terms of the large cell densities cultured in the PCNMs, further analysis is warranted to better understand the effects of the fabrication process on MG-63 function and phenotype.

To assess the morphology of cells adhered onto PCNMs films, the materials were seeded with MG-63 osteosarcoma cells. After 3 days of culturing, the cells on the PCNMs films were labeled with fluorescence dye. The morphology of the cells cultured on the materials maintained oval shapes [Fig. 8(a)]. Immunofluorescence staining for filamentous actin (red color) and vinculin, a cytoskeletal protein (green color) dyed with rhodamine-labeled phalloidin and anti-vinculin antibody followed by alexa-fluoro 488 rabbit antimouse IgG, respectively. Actin fibers and vinculin protein, were clearly observed in the cells adhered onto the PCNMs films.

These results support that PLGA and marine collagen are functionally active promoting cell adhesion and spreading of normal human epithelial cell onto the PLGA/collagen nanofibrous membrane.

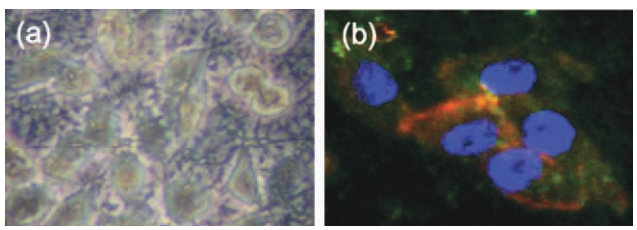

Figure 8 Morphologies and immune-fluorescence dye staining of MG-63 osteoblastic cells adherent on the PCNMs films. The materials were seed with MG-63 osteosarcoma cells. After 3 days of culture, the cells were labeled with fluorescence dye; (a) optical microscope image and (b) immune-fluorescent staining image. [Color figure can be viewed in the online issue, which is available at wileyonlinelibrary.com.]

CONCLUSION

PCNMs have been successfully prepared by electrospinning of PLGA/collagen solutions. The morphology of the electrospun fibers was strongly affected by parameters such as polymer concentration, PLGA/collagen ratio, applied voltage, flow rate, and

needle tip diameter. By increasing the applied electric field, the morphology was changed from a beaded fiber to a uniform fiber structure and the fiber diameter was also increased. There was an increase in the average fiber diameter with an increase in the concentration of the polymer solution, PLGA ratio, flow rate, and needle tip diameter. We confirmed that the PCNMs accommodated the survival and proliferation of MG-63. MG-63 apparently attached to the PLGA/collagen nanofibers, and showed apparently different morphological features.

References

1. Langer, R.; Vacanti, J. P. Science 1993, 260, 920.
2. Badylak, S. F. Clin Tech Equine Pract 2004, 3, 173.
3. Kim, K.; Yu, M.; Zong, X.; Chiu, J.; Fang, D.; Seo, Y. S. Biomaterials 2003, 24, 4977.
4. Metzke, M.; O'Connor, N.; Maiti, S.; Nelson, E.; Guan, Z. Angew Chem Int Ed 2005, 44, 652.
5. Boland, E. D.; Matthews, J. A.; Pawlowski, K. J.; Simpson, D. G.; Wnek, G. E. Bowlin, G. L. Front Biosci 2004, 9, 1422.
6. Riboldi, S. A.; Sampaolesi, M.; Neuenschwander, P.; Cossu, G.; Mantero, S. Biomaterials 2005, 26, 4606.
7. Khil, M. S.; Cha, D. I.; Kim, H. Y.; Kim, I. S.; Bhattarai, N. J Biomed Mater Res B Appl Biomater 2003, 67, 675.
8. Zeng, J.; Yang, L.; Liang, Q.; Zhang, X.; Guan, H.; Xu, X. J Controlled Release 2005, 105, 43.
9. Buttafoco, L.; Kolkman, N. G.; Poot, A.; Dijkstra, P. J.; Vermes, I.; Feijen, J. J Controlled Release 2005, 101, 322.
10. Fong, H.; Chun, I.; Reneker, D. H. Polymer 1999, 40, 4585.
11. Hutmacher, D. W.; Schantz, T.; Zein, I.; Ng, K. W.; Teoh, S. H.; Tan, K. C. J Biomed Mater Res 2001, 55, 203.
12. Williamson, M. R.; Coombes, A. G. Biomaterials 2004, 25, 459.
13. Ma, P. X. Mater Today 2004, 7, 30.
14. Matthews, J. A.; Wnek, G. E.; Simpson, D. G.; Bowlin, G. L. Biomacromolecules 2002, 3, 232.
15. Buttafoco, L.; Kolkman N. G.; Engbers-Buijtenhuijs, P.; Poot, A. A.; Dijkstra P. J.; Vermes, I.; Feijen, J. Biomaterials 2006, 27, 724.
16. Dong, B.; Arnoult, O.; Smith, M. E.; Wnek, G. E. Macromol Rapid Commun 2009, 30, 539.
17. Song, E.; Kim, S. Y.; Chun, T. H.; Byun, H. J.; Lee, Y. M. Biomaterials 2006, 27, 2951.
18. Shin, Y. M.; Kim, K. S.; Lim, Y. M.; Nho, Y. C.; Shin, H. S. Biomacromolecules 2008, 9, 1772.
19. Hozumi, K. T.; Yamagata, N.; Otagiri, D.; Fujimori, C.; Kikkawa, Y.; Kadoya, Y.; Nomizu, M. Biomaterials 2009, 30, 1596.
20. Diener, A.; Nebe, B.; Luthen, F.; Becker, P.; Beck, U.; Neumann, H. G.; Rychly, J. Biomaterials 2005, 26, 383.
21. Rho, K. S.; Jeong, L.; Lee G.; Seo, B. M.; Park, Y. J.; Hong, S. D.; Roh, S.; Cho, J. J.; Park, W. H.; Min, M. B. Biomaterials 2006, 27, 1452.
22. Kim, S. J.; Jang, D. H.; Park, W. H.; Min, B. M. Polymer 2010, 51, 1320.
23. Huang, L.; Nagapudi, K, Apkarian, R. P.; Chaikof, E. L. J Biomater Sci Polym Ed 2001, 22, 1737.
24. Xin, X.; Hussain, M.; Mao, J. J. Biomaterials 2007, 28, 316.
25. Pham, Q. P.; Sharma U.; Mikos, A. G. Tissue Eng 2006, 12, 1197.